Performance evaluation of compound parabolic solar collector using different nanofluids: An experimental study

Muhammad Farhan[1], Muhammad Ihsan Shahid[1], Furqan Jamil[2], Muhammad Usman[3], M. A. Mujtaba[3]*, Muhammad Wajid Saleem[4], Syed Nasir Shah[5], Shahid Saghir[1], Abdulfatah Abdu Yusuf[6], Mohamed Mousa[7] and A.S. El-Shafay[8,9]

[1]Mechanical Engineering Department, University of Management and Technology, Sialkot Campus, Lahore, Pakistan, [2]Mechanical Engineering Department, University of Wah, Wah Cantonment, Pakistan, [3]Department of Mechanical Engineering, University of Engineering and Technology Lahore, Lahore, Pakistan, [4]Department of Mechanical and Mechatronics Engineering, College of Engineering, Dhofar University Salalah, Salalah, Oman, [5]Energy Engineering Department, University of Engineering and Technology, Taxila, Pakistan, [6]Department of Mechanical Engineering, Kampala International University, Ishaka, Uganda, [7]Electrical Engineering Department, Faculty of Engineering and Technology, Future University in Egypt, New Cairo, Egypt, [8]Department of Mechanical Engineering, College of Engineering, Prince Sattam Bin Abdulaziz University, Alkharj, Saudi Arabia, [9]Mechanical Power Engineering Department, Faculty of Engineering, Mansoura University, Mansoura, Egypt

The article reports an experimental study on a non-tracking compound parabolic collector (CPC) with nanofluid and hybrid nanofluids (NFs). An experimental setup was fabricated having a concentration ratio of 4.17, 0.828 m^2 collector area, 24° of half acceptance angle, and an evacuated tube receiver having 1.85 m length. Fluids like water and NFs have been investigated in CPC performance improvement, but current research deals with NFs and hybrid NFs in a CPC as rare studies are found on a CPC using NFs. The 0.010 and 0.015 wt% concentration were used of nanofluids (NFs) which were silica/water + ethylene glycol (SiO_2)/(H_2O + EG), and hybrid nanofluids of magnesium oxide + carbon black/water (MgO + CB/H_2O) and carbon black + graphene nanoplatelets/water (CB + GNPs/H_2O) at flow rates of 0.020, 0.015, and 0.010 kg/s. The experimentation was performed under real climate conditions of Taxila, Pakistan, and solar irradiance and ambient temperature were measured to determine the performance of the CPC in comparison to a simple base fluid which was water. The experimental results revealed that a maximum temperature difference of 8.5°C with an around thermal efficiency of 38.51% was achieved for hybrid pair of MgO + CB at a flow rate of 0.010 kg/s and volumetric concentration of 0.015 wt%. The efficiency variation using NFs (SiO_2/EG + H_2O) varies from 12.8% to 59.1% from lowest 0.010 kg/s to highest 0.020 kg/s flow rates, and volumetric concentrations (0.010 and 0.015 wt%) of nanoparticles. For similar experimental conditions, efficiency variation for (CB + GNPs) pair varies from 14.2% to 65.6% for aforementioned conditions. Efficiency variation from 15.3% to 66.3% was attained using MgO + CB in the base fluid of water for said flow rates and

volumetric concentrations of nanoparticles. In addition, an efficiency enhancement of 24.3%, 30.8%, and 31.5% was observed for $SiO_2/EG + H_2O$, $CB + GNPs/H_2O$, and $MgO + CB/H_2O$, respectively, at maximum flow rates and volumetric concentration of nanoparticles as compared to water. Therefore, the usage of hybrid-based NF in the CPC is beneficial in terms of efficiency enhancement, and it will bring young research workers to get deep into this field to bring revolution in the area of solar energy.

Introduction

The escalating rate of fossil fuel depletion, global warming, and growing energy demands can be proficiently faced by utilizing solar energy (Tiwari and Tiwari, 2017; Xu and Wang, 2017; Dimri et al., 2018). Solar energy is an abundantly available energy source which can be converted either to electricity (with PV) or to useful heat (with thermal collectors) (Korres and Tzivanidis, 2018; Subramani et al., 2018). A potential design to enhance the efficiency of solar collectors is incorporating the concept of concentration. Compound parabolic collectors (CPCs) are efficient concentrating solar collectors due to their ability for producing hot temperature-based water, and thus, they are mostly suited for domestic hot water applications. Furthermore, even when sun rays do not strike the collector at an optimized angle, they can still maintain water at a high temperature without a tracking system. This reason makes the CPC a potential candidate as a more efficient solar collector for low-temperature applications (Gilani and Hoseinzadeh, 2021). Verma et al. (2018) identified that one of the paramount sources of sustainable energy is solar energy, which is abundantly available in almost all areas in South Asia having a potential of about 2.9 million MW without disturbing the environmental conditions. Ghafoor et al. (2016) analyzed in the country of Pakistan that about 30% of the energy is utilized by the construction sector yearly. Thus, the literature demonstrates the increase in energy utilization to overcome energy demand.

Kim et al. (2013) investigated several residential and industrial practices working in the intermediate temperature (100°C–300°C) range accompanied by various solar thermal collectors. Various daily use applications such as solar stills, extraction of oil, generation of electricity at a small level, textile, and food industry technology mandate energy fonts in the abovementioned low to medium range temperatures. Hachicha et al. (2013) as well as Li et al. (2017) investigated flat plate collectors in a low temperature range, while concentrating ones were considered for the medium temperature range. Bellos and Tzivanidis (2019) analyzed that the CPC is suitable for medium temperature ranges in diverse applications. Snail et al. (1984) and Ayompe et al. (2011) examined a non-tracking CPC with an evacuated tube and found 50% thermal effectiveness and 65% optical performance. Jiang et al. (2020) analyzed the tubular absorber CPC and found that it is efficient, systematic, and diverse especially appropriate for industrial and other medium-temperature applications. Gilani and Hoseinzadeh (2021) investigated CPC advantages over flat plate solar collectors in terms of power production, cost-effectiveness, and CO_2 reduction. Ayompe et al. (2011) and Snail et al. (1984) studied a tracking system with a solar thermal collector and concluded that improvement in the overall efficiency of the system was carried out. Detailed investigation revealed the 15% better results achieved by accompanying the tracking system with solar collectors. Oloketuyi et al. (2020) investigated the hybrid compound parabolic collector (HCPC) both experimentally and mathematically for refrigeration purposes. Numerical results showed that for attaining 70°C–85°C desorption temperature, 350–450 W/m^2 solar radiation intensity was required. Acosta-Herazo et al. (2020) investigated the CPC photoreactor's absorption performance for solar radiation by changing several variables and found the boundary wall of the receiver has a considerable effect on the performance of CPCs. Leong et al. (2018) experimentally investigated copper and titania NFs by varying particle concentrations, surfactants, sonication time, and pH value. PVP surfactants and neutral base fluids exhibited higher values of thermal conductivity at higher volumetric concentrations of nanoparticles in base fluids. Vijayakumar et al. (2021) investigated that by using NFs in CPCs, thermal performance and efficiency of the system enhance significantly. Bhalla and Khullar analyzed to improve the performance and efficiency of solar collectors without a tracking system; non-imaging concentrators along with advanced working fluids can be employed. In the current work, a nanofluid-based receiver is employed in a non-imaging concentrator CPC to enhance the thermal performance of the collector (Bhalla and Khullar, 2021). Harrabi et al. (2021) investigated NFs in different solar collectors and found thermal performance enhancement by the use of NFs. The payback period was reduced by 0.62 years as compared to mineral thermal oil by using 0.3% MWCNT/oil in CPCs.

Hybrid NFs exhibited an increased heat transfer rate owing to enhanced thermal conductivity as compared to simple NFs.

The hybrid NFs have high density, viscosity, and thermal conductivity as compared to the base fluid, but have lower specific heat capacity. Higher thermal conductivity is one of the core advantages of hybrid NFs, but greater viscosity is one of the limitations of hybrid NFs. The product of specific heat capacity and density represents the quantity of heat that fluid can transport. The product is generally high for the hybrid NFs as compared to the base fluid; hence, the NFs are the ideal heat transfer fluid. Takabi and Salehi (2014) investigated hybrid NFs by dispersing nanosized particles of various metals and non-metals in different base fluids. Different thermal properties were obtained by using different volumetric concentrations. Sundar et al. (2014) measured and found that the stability of hybrid NFs in most cases is not exceeding more than 15 days by employing direct and indirect enhancement methods. Toghraie et al. (2016) investigated that by increasing temperature and volumetric concentrations, the thermal conductivity of hybrid NFs increases. Zeng and Xuan (2018) experimentally investigated Ag/SiO_2 and MWCNT's and found that a hybrid of these yielded 5.4% and 1.3% enhanced results than unitary ones of Ag, SiO_2, and MWCNT's correspondingly. Chen et al. (2017) experimentally analyzed ATO-CuO hybrid NFs and found a hybrid of these (99.6% absorption fraction of solar irradiations) and mono of each have 89.8% and 89.5% correspondingly. Solar thermal efficiency of hybrid NFs was 92.5%, whereas NFs have 80.7% and 81.3% correspondingly. Campos et al. (2019) carried out a simulation study and found that a silver and graphene oxide combined unit has 20% greater system efficiency than an individual of each. Amjad et al. (2018) investigated the use of nanofluids in water desalination.

Farajzadeh et al. (2018) investigated a flat plate solar collector (FPSC) experimentally and numerically using Al_2O_3 and TiO_2 NFs, and found efficiency enhancement of 19% and 21% correspondingly. Under similar experimental conditions, a hybrid of Al_2O_3 and TiO_2 yielded a 26% efficiency enhancement. Amjad et al. (2017a) investigated steam production by using gold-based nanofluids. Bellos and Tzivanidis (2018) experimentally investigated a parabolic trough collector (PTC) by using mono (Al_2O_3/Oil and TiO_2/Oil) and hybrid NFs ($Al_2O_3 + TiO_2$/Oil). Hybrid NFs enhanced 0.74% efficiency, and mono of each enhanced 0.34% and 0.341% correspondingly under similar experimental conditions. Chen et al. (2016) investigated the photothermal conversion efficiency of mono (Au, Ag in water) and hybrid (Au + Ag)/H_2O NFs and found that hybrid NFs have nearly 30.97% efficiency than mono ones (11.90% + 19.01%) correspondingly. Menbari et al. (2017) experimentally analyzed Al_2O_3 + CuO/water in a direct absorption solar collector (DASC) and found that enhancement in efficiency by hybrid nanofluid is higher than that in NFs under similar experimental conditions. Qamar et al. (2021) investigated the dispersion stability of ZnO-based nanofluids. The performance of solar collectors has been thoroughly investigated by varying solar collector materials

under similar climatic conditions by Belkhode et al. (2021). Ahmadi et al. (2021) performed energy and exergy analysis on Agro-product drying technologies powered by solar energy. Discussion on applications of tracked and non-tracked solar thermal collectors and their limitations were also discussed by Ahmadi et al. (2020). Amjad et al. (2017b) studied the effect of hybrid nanofluids in direct absorption. Khalil et al. (2020) investigated the performance of hybrid nanofluids in parabolic trough collectors. The summary of various hybrid NFs in different applications is summarized in Table 1.

Several studies have been (Chen et al., 2016; Menbari et al., 2016; Toghraie et al., 2016; Amjad et al., 2017a; Amjad et al., 2017b; Chen et al., 2017; Menbari et al., 2017; Amjad et al., 2018; Bellos and Tzivanidis, 2018; Farajzadeh et al., 2018; Wang et al., 2018; Zeng and Xuan, 2018; Campos et al., 2019; Ahmadi et al., 2020; Khalil et al., 2020; Ahmadi et al., 2021; Belkhode et al., 2021; Qamar et al., 2021) carried out in the literature on the use of hybrid NFs in various solar collectors for efficiency improvements. Critical analysis of the literature reveals that numbers of studies are available for parabolic collectors using different NFs in various solar collectors, but the rare study was found on CPCs using hybrid-based NFs. Therefore, in the present work, the solar CPC system is experimentally investigated with SiO_2/H_2O + EG nanofluids and hybrid NFs of $MgO + CB/H_2O$ and $CB + GNPs/H_2O$. Nanofluids and hybrid NFs at two different volumetric concentrations and three different mass flow rates are experimentally analyzed in the current work, and a comparison is done with base fluid water in order to measure the enhancement of CPC efficiency. Thus, this research will attract young research workers who are working on the thermal management of CPC. An experimental investigation will be carried out by keeping in view objectives like the selection and preparation of nanoparticles and their potential evaluation in CPC setups under real climatic conditions.

Preparation of nanofluids and hybrid nanofluids

In the preparation of NFs and hybrid NFs, stabilization of nanoparticles in the respective base fluid is always a difficult task owing to the presence of cohesive and van der Waals forces. In several studies, a two-step method was used for NF preparation in which particle preparation and dispersion in base fluid were carried out separately. To avoid the sedimentation of nanoparticles, several additional techniques like ultrasonication, surfactant addition, and high-pressure homogenization may be adopted (Babar and Ali, 2019). Suresh et al. (2011) used a two-step method to prepare Al_2O_3–Cu/water with various particle concentrations. A specific amount of sodium lauryl sulfate and Al_2O_3–Cu nanoparticles were suspended in the base fluid along with

TABLE 1 Summary of various investigators on various hybrid NFs in different applications.

Hybrid nanoparticles	Base fluid	Concentration of particles	Solar system	Findings	References
Al$_2$O$_3$–TiO2	Water	0.1 wt%	FPSC	Hybrid NFs depicted more efficiency enhancement than unitary ones.	Farajzadeh et al. (2018)
Gold–silver	Water	1.75 ppm Au—0.15 ppm Ag	DASC	Photothermal conversion efficiency of hybrid particles is found to be more efficient than that of unitary ones for the same experimental conditions.	Chen et al. (2016)
CuO–γ Al$_2$O$_3$	Water, EG	Not fixed	DASC	Hybrid NFs were more efficient than the unitary of any of these in DASC.	Menbari et al. (2016)
Ag–ZnO	Silicone Oil	1.0 mg/ml	DASC	240% photothermal efficiency enhancement was observed in comparison to base fluid for hybrid NFs.	Wang et al. (2018)
Sn–SiO$_2$–Ag	Water	0.01–0.05 vol%	DASC	By utilizing hybrid NFs, considerable efficiency enhancement was observed as compared to unitary and base fluids.	Zeng et al. (2016)
Co-C/therminol	Therminol	—	DASC	Considerable efficiency enhancement was observed by employing hybrid NFs	Ahmadi et al. (2021)
SiC-PCM	Water	SiC: 0.1% mass fraction	Photovoltaic/ thermal (PV/T)	Thermal efficiency enhancement was observed by employing hybrid NF in PV/T.	Al-Waeli et al. (2017)
Al$_2$O$_3$–ZnO	Water	0.5%	PV/T	Exergy and energy efficiency enhancement was observed by utilizing hybrid NFs as compared to NFs.	Younis et al. (2018)
Cu–TiO$_2$	Water	0.2 wt%	PV/T	5.84% thermal efficiency enhancement was noted as compared to base fluids for the same experimental conditions.	Sathieshkumar, (2018)
Ag–SiO$_2$–CNT	Water	0.006 wt% (Ag-SiO2) 0.067 wt% CNT	PV/T	Considerable increase in thermal and electrical efficiency observed by incorporating hybrid NFs in PV/T setup.	Hjerrild et al. (2016)
Ag–SiO$_2$	Water	0.0205 wt%	PV/T	12% increase in energy scattering ability was noted by using hybrid NFs as compared to base fluids.	Crisostomo et al. (2017)
CuO/Sylterm 800	Sylterm 800	5% by volume	CPC	Nanofluid utilization in the system increases the flow heat transfer coefficient by 17.41% and 15.53% for high and low operating temperatures, respectively.	Korres et al. (2019)

TABLE 2 Recent work on various hybrid NFs.

Hybrid nanofluid	Sonication time (h)	Magnetic stirring (h)	Stability (days)	Investigator
Al$_2$O$_3$–Ag/water	0.5	—	2	Allahyar et al. (2016)
Cu–TiO$_2$/water and EG	6	3	7	Esfe et al. (2015)
TiO$_2$–SiO$_2$/water and EG	2	1	14	Hamid et al. (2018)
MWCNTs–ZnO/water and EG	3	2	10	Esfe et al. (2017)

ultrasonication to avoid cluster formation. Parsian and Akbari (2018) prepared a hybrid nanofluid of Al$_2$O$_3$–Cu/EG using a two-step method. Nanoparticles in a specific amount dispersed in base fluid and the solution was sonicated for 7 h to stabilize the solution, and the solution remained stable for 3 days. The summary of various hybrid NFs studies by various authors is summarized in Table 2.

In this study, various nanosized particles are used in a solar collector system for thermal enhancement. Extremely pure nanosized particles were used which were carbon black, graphene nanoplatelets, and magnesium oxide (shown in Figure 1) that were purchased from Nanostructured and Amorphous Materials, Inc., Houston, United States and Advanced Chemical Supplier Material LLC, Pasadena, CA. The TEM images of the particles are given in Figure 2.

Nanosized particles were mixed with different base fluids in different ways. The method used to prepare NFs and hybrid NFs was a two-step method. At the start, a specific concentration of granular nanoparticles was dispersed in base fluids. Homogenizer was used for stirring purposes at 6,000–8,500 rpm; stirring at a higher frequency led to rupturing of grains of nanoparticles to thoroughly blend them into the base fluid. After that, an ultrasonic vibrator was used to break covalent bonds among particles. The sonication of

FIGURE 1
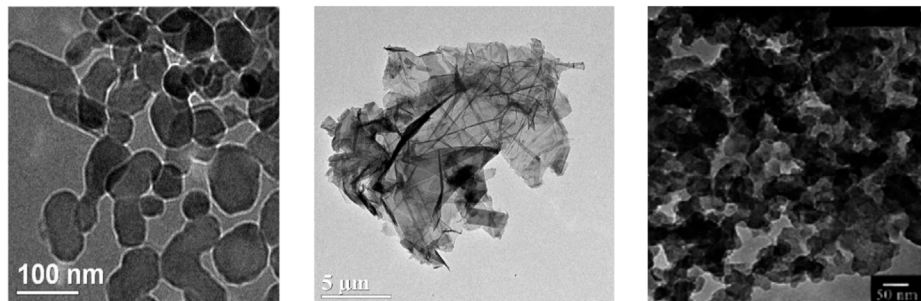**(A)** Carbon black NPs, **(B)** graphene nanoplatelets, and **(C)** MgO nanoparticles.

FIGURE 2
TEM image of MgO (left), graphene nanoplatelets (middle), and carbon black (right) (Courtesy: Nanostructured and Amorphous Materials, Inc., Houston, United States; Advanced Chemical Supplier Material LLC, Pasadena, CA, United States).

nanofluid and hybrid NFs reduces the mixture space and thoroughly homogenized it. Sonication of NFs was done for 3–4 (SiO_2/H_2O + EG) hours and 5–6 h for MGO + CB and CB + GNPs for hybrid NFs in the base fluid of water so that the mixture may stabilize.

A simple flow diagram for the preparation of nanofluid and hybrid NFs is illustrated in Figure 3. The prepared NFs and hybrid NFs are shown in Figure 4.

The stability of nanofluid and hybrid nanofluid was thoroughly observed, and no sedimentation of particles was found in 9 days after their preparations. The stable NFs and hybrid nanofluids are shown in Figure 5.
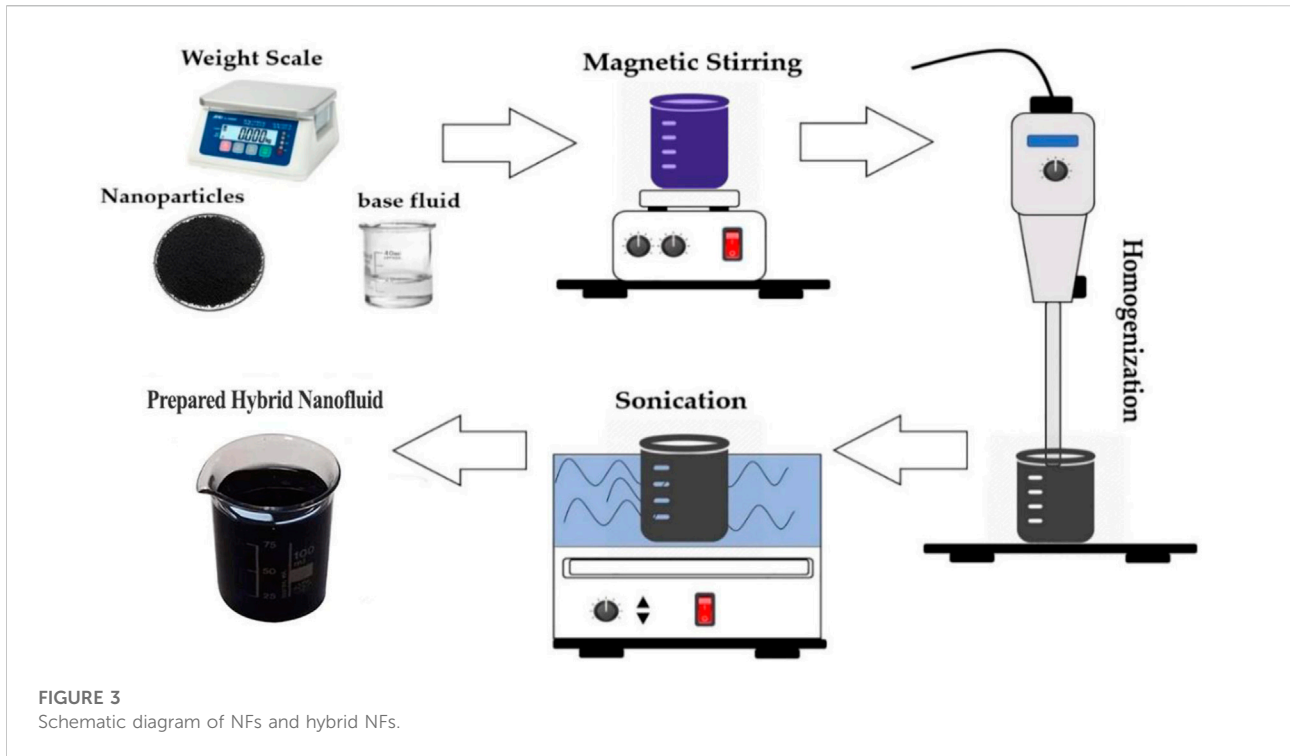
Experimental setup

The experimental setup was installed at the Energy Engineering Department of University of Engineering and Technology, Taxila, Pakistan. For the present experimental setup, the direction of the compound parabolic solar collector was demarcated by the solar pathfinder. The pathfinder identified

all directions in a circle dome for the selection of solar collector orientation. It identifies the tree and building shadows, the intensity of radiations, and the direction of the collector along the axes.

The system schematic diagram is shown in Figure 6. It explains the flow of fluids and observation of flow rate by a flow meter and measurement of temperature at the inlet and outlet of CPSC.

Experimental methodology

An experimental study was carried out by using water nanofluids and hybrid NFs, that is, SiO_2 in the hybrid base fluid of water and ethylene glycol, MgO + CB and CB + GNPs in distilled water as base fluid. The experimentation was carried out to check the thermal performance of the compound parabolic collector for real climatic conditions of Taxila, Pakistan. The geographical location of Taxila has a latitude of 33.74°N and a longitude as 72.78°E. NFs and hybrid NFs were prepared by the two-step method *via* using a homogenizer and

FIGURE 3
Schematic diagram of NFs and hybrid NFs.

FIGURE 4
Prepared NFs and hybrid NFs: **(A)** MgO + CB/water, **(B)** MgO + CB/water, **(C)** SiO$_2$/water + EG, **(D)** SiO$_2$/water + EG, **(E)** CB + GNPs, and **(F)** CB + GNPs.

ultrasonic vibrator. The variation in results for both configurations at different flow rates (0.01, 0.015, and 0.020 kg/s) and volumetric concentrations (0.010 and 0.015 wt%) of NFs and hybrid NFs were examined. The experimentation was done in October–November 2020. The time for experimentation was 10:00 a.m. to 3:00 p.m. on a daily
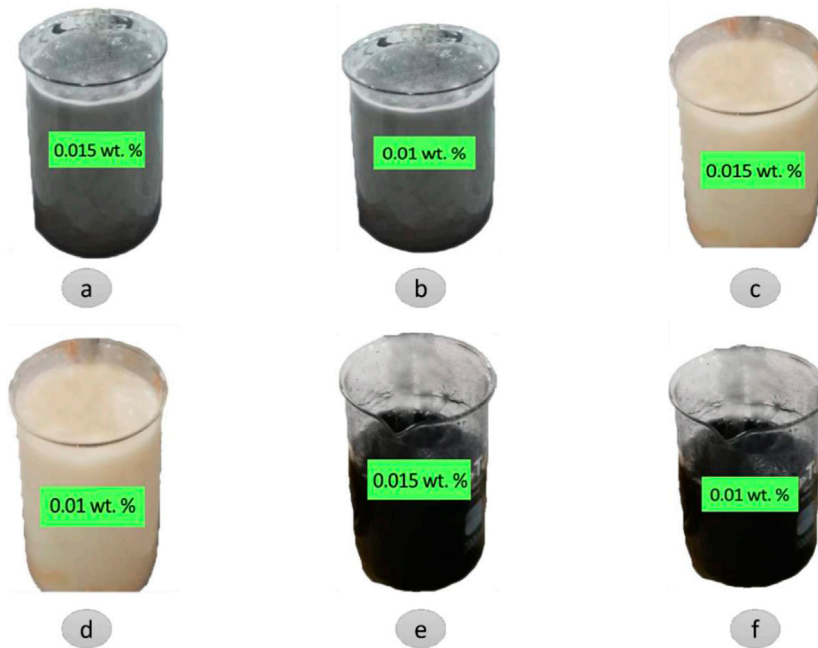
FIGURE 5
Stable NFs and hybrid NFs after 9 days: **(A)** CB + MgO, **(B)** CB + MgO, **(C)** SiO_2/water + EG, **(D)** SiO_2/water + EG, **(E)** CB + GNPs, and **(F)** CB + GNPs.
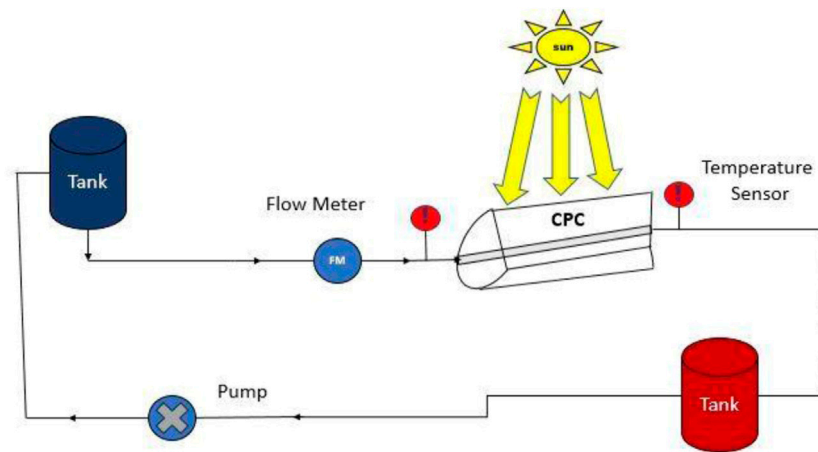

FIGURE 6
System schematic diagram.

basis for moderate weather of Taxila. The experimental setup made of the close loop to examine the thermal efficiency of CPSC setup at some specific properties and operating conditions for water, nanofluids, and hybrid NFs. First, the leakage at every point is tested and the proper flow rate was set. Cold water/NFs/hybrid NFs enter from the pump to the compound parabolic solar collector which heats up water/NFs/hybrid NFs. For steady output, high-temperature water from the collector enters the storage tank. The normal water from the outside of the tank goes toward the source side. In this way, the loop continues. To check the temperatures at the inlet and outlet valves, sensors were installed with great care. The

K-type thermocouples (5 TC-TT-KI-24-2M, Omega United States) having an uncertainty of ±0.1°C were used to measure the temperature. The flow rate for H_2O, NFs, and hybrid NFs is measured by a flow meter installed at the inlet port. A flow rate measuring sensor (OKY3430-0) having a measuring range from 1 to 30 L/min was used to measure the flow rate. Wind velocity was recorded by anemometer with an uncertainty range of 200–3,000 ns. A pyranometer is used to measure hourly solar radiations. A fiber optic temperature sensor is used to measure ambient temperature. After every 15 min, experimental readings are measured, but the hourly values show the average readings. To assure accuracy, values are repeated at the same flow rate and concentrations of fluids for 2 days. As the solar rays reach the compound parabolic collector, it reflects these radiations to a focus line made by the receiver. The angle of incidence for coming radiations is important to reflect maximum solar radiations. The water passes from the inlet valve to the solar collector and removes by the outlet temperature valve. The collector temperature at these two valves is measured by thermometers. The outlet water goes to a hot thermal storage tank for steady flow. Water, NFs, and hybrid NFs are continued in the loop of water heating by the solar system. To avoid consolidation and ensure stability, NFs and hybrid NFs re-blended and homogenized every morning. Energy potential (Q_s), heat gain (Q_u), and thermal efficiency (η_{th}) of CPSC can be calculated by using Eqs 1–3 (Bellos et al., 2016):

$$Q_s = A_a.G_e, \tag{1}$$

where A_a is the area of the absorber tube and G_e is the incident solar irradiance on the collector.

$$Q_u = m.C_p.(T_{out} - T_{in}), \tag{2}$$

where m is the mass flow rate of fluid and C_p is the specific heat capacity of working fluid.

Thermal efficiency (η_{th}) of CPSC can be calculated by using

$$\eta_{th} = \frac{Q_u}{Q_s}, \tag{3}$$

Results and discussion

In this section, the experimentation is carried out for Taxila climate under real conditions. The ambient temperature varies from 22.5°C to 26.8°C. The solar radiations are captured by a pyranometer whose maximum ranges go to 1220 W/m², while the collector inlet and outlet temperatures are measured with a fiber optic heat transfer temperature sensor. The experimentation is carried out with four fluids, that is, water, NFs, and two concentrations of hybrid NFs. The timing for experimentation was set as 10:00 a.m. to 3:00 p.m.

Validation of experimental setup

The accuracy of the experimental setup was validated by comparing the heat gain of CPCs with the published work of Akhtar et al. (2020). Figure 7 represents the comparison b/w current work and published work. Experimentation of the published work was performed in March to May, while current experimentation is conducted in September to November under the real climatic condition of Taxila. The overall pattern of heat gain is similar at a similar flow rate; however, variations in starting, optimum, and ending points are due to seasonal variations.

Climate conditions

The present work basically shows a comparison of the thermal enhancement of nanofluids and hybrid nanofluids as compared to water. As this system is used for low–medium range temperature applications, the average outlet temperature achieved from the collector is 45°C–53°C. From the experimentation, it is concluded that the minimum radiations gained by the ambient condition of Taxila are 4.5 kWh/m²/day. The average peak hours of weather gave solar radiation as 6.1 kWh/m². From the average look of annually solar irradiance, the existing radiation are higher than the minimum requirements for solar potential applications. Figure 8 predicts the environmental conditions of Taxila, Pakistan. The annual trend of the model shows the ambient temperature and wind velocity. The overall impact of temperature changes from 22.5°C to 26.8°C.

The average solar radiation measured through scenarios for 6 h are shown in Figure 9. The intensity of radiation depends upon different factors which reduce its irradiance. The clouds, dust, humidity, and wind velocity are those factors that influence the intensity of radiation. The increase in ambient temperature is roughly proportional to the removal of humidity and high radiations. These climatic parameters affect the solar collector output and system efficiency.

Effect of efficiency with time, flow rate, and concentration of nanoparticles using water nanofluids and hybrid nanofluids

The experimental outcomes conclude that the thermal analysis is mainly dependent on the thermal efficiency attained by the solar thermal collector. Average values taken for figures at similar test conditions are considered. The thermal efficiency indicates the overall performance of the solar thermal collector which directly changes with the intensity of solar radiations. At constant flow rate and weather
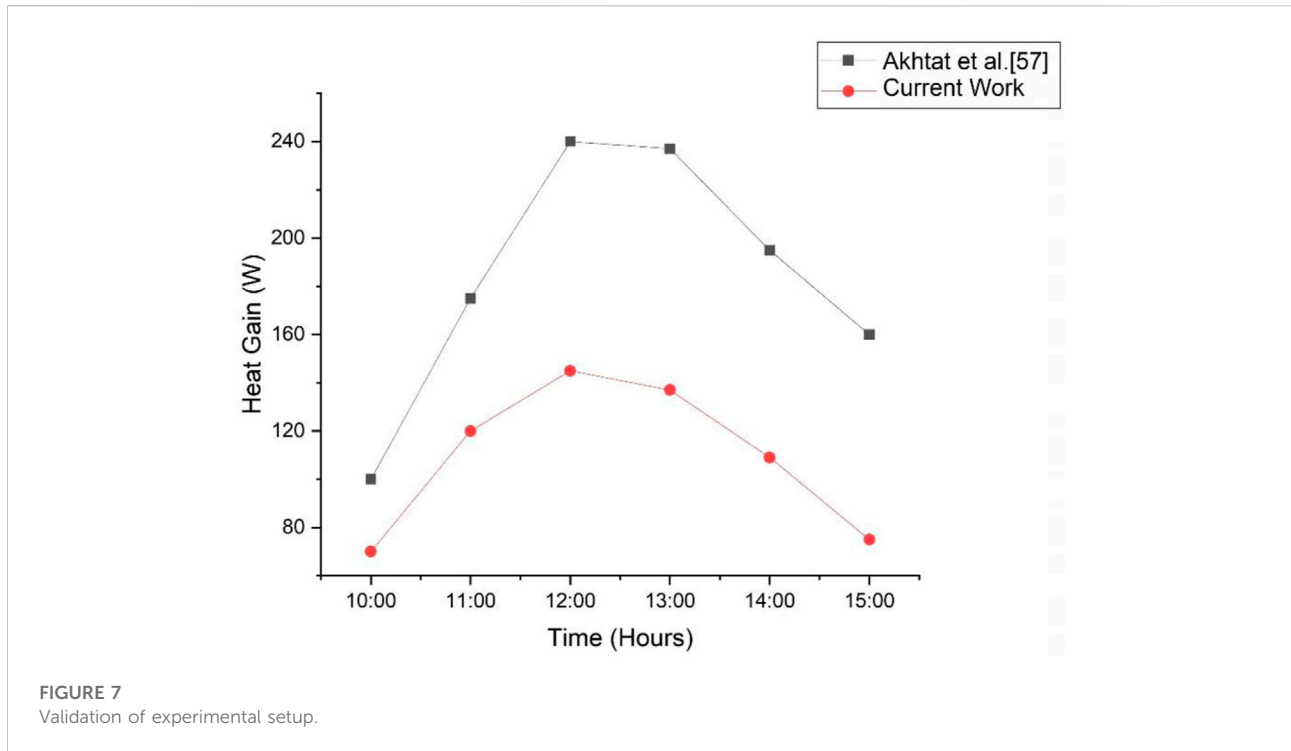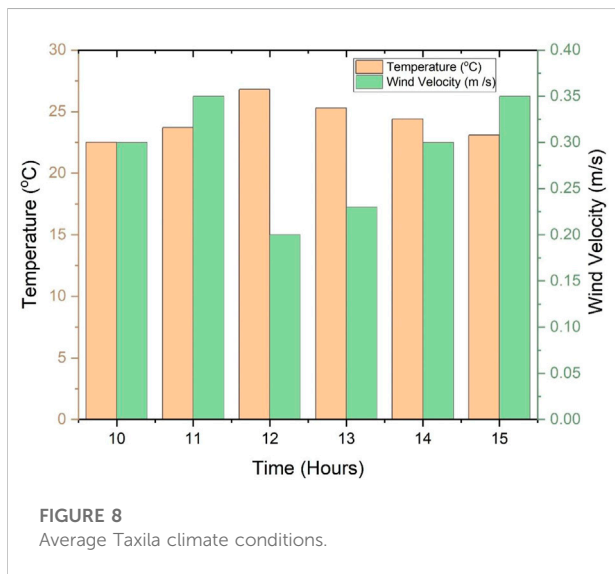
FIGURE 7
Validation of experimental setup.

FIGURE 8
Average Taxila climate conditions.

difference decreases with the increase of flow, and efficiency increases with flow rate. This direct and inverse relation is the main drive for variation of graphs. The efficiency achieved using NFs of (SiO_2/EG + H_2O) varies from 20.8% to 59.13% for Taxila climate. For same climatic conditions, efficiency for hybrid NFs (CB + GNPs) varies from 14.2% to 65.68%. Efficiency varies from 15.3% to 66.36% by using hybrid NFs of MgO + CB in the base fluid of water at higher concentration and flow rate.

Effect of solar heat gain with time, flow rate, and concentration of nanoparticles using water, nanofluids, and hybrid nanofluids

The solar heat gain varies with the specific heat capacity of fluids and temperature difference at different concentration ratios and flow rates. Average values taken for figures at similar test conditions are considered. The variation of water NFs and two concentrations of hybrid NFs are shown in Figure 11. The hybrid NFs gave 31.5% improved results than simple base fluid water.

From Figures 11A–D, it is obvious that due to the variation in particle concentration, the trend of solar heat gain and other parameters also varies accordingly. The solar heat gain changes from 77.85 to 470 W at a lower flow of

conditions, the thermal performance of CPC increases due to the enhanced surface area and thermal properties of nanoparticles and hybrid nanoparticles.

From Figures 10A–D, it is obvious that due to the variation in particle concentration, the trend of thermal efficiency and other parameters also varies accordingly. The efficiency of water improved from 12.5% to 34.8%. The variation increases with an increase in the flow rate; no doubt the temperature
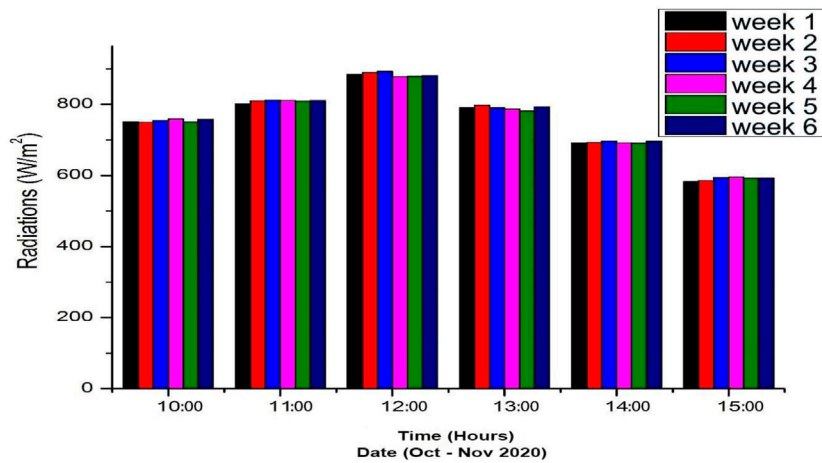
FIGURE 9
Average solar radiation data.
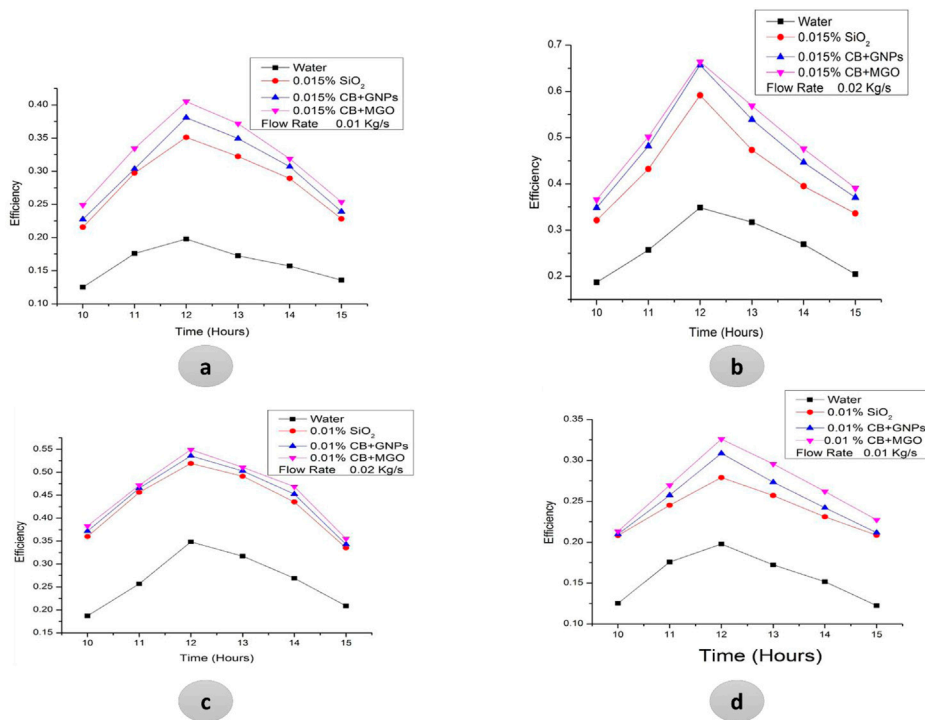
FIGURE 10
Efficiency at different flow rates with different concentrations of NFs and hybrid NFs. **(A)** 0.01 kg/s, with 0.015 wt% concentration of NFs and hybrid NFs. **(B)** 0.020 kg/s, with 0.015 wt% concentration of NFs and hybrid NFs. **(C)** for 0.020 kg/s and 0.010 wt% concentration of NFs and hybrid NFs. **(D)** 0.010 kg/sand 0.010 wt% concentration of NFs and hybrid NFs.

0.01 kg/s to the highest flow of 0.020 kg/s for water and hybrid NFs (MgO + CB/water), respectively. At such a high flow rate, the solar gain and efficiency were high, but the temperature difference will be minimum as compared to the remaining flow rates. The maximum solar gain is achieved at high concentration and the flow rate was 470 W.

FIGURE 11
Solar heat gain received by CPCs at different flow rates for different concentrations of NFs and hybrid NFs for Taxila climate. **(A)** 0.010 kg/sand 0.015 wt% flow rate and concentration of NFs and hybrid NFs, respectively. **(B)** 0.01 kg/s flow rate and 0.010 wt% concentration of NFs and hybrid NFs. **(C)** 0.020 kg/s flow rate and 0.015 wt% concentration of NFs and hybrid NFs. **(D)** 0.020 kg/s flow rate and 0.010 wt% concentration of NFs and hybrid NFs.

Temperature difference with time, flow rate, and concentration of nanoparticles using water, nanofluids, and hybrid nanofluids

The line graph in Figure 12 indicates the variation of temperature difference at three different flow rates. Average values taken for figures at similar test conditions are considered.

From Figures 12A–D, it is obvious that due to the variation in particle concentration, the trend of the temperature difference and other parameters also varies accordingly. For water, variation in temperature is 1.4°C–3.4°C for higher to lowest flow rates. While at the same climate conditions, the NFs (hybrid base fluid EG + water and nanoparticles of SiO_2) gave improved results at 2°C–7.8°C, respectively. This range varies from 2.1°C to 7.7°C for CB + GNPs in the base fluid of water. For hybrid NFs of CB + MgO, this range varies from 2.4°C to 8.5°C for higher to lowest flow rates, respectively.

Compound parabolic collector comparison at different flow rates for nanofluids and hybrid nanofluids

In Figure 13, the comparison is carried out for two concentrations of NFs and hybrid NFs at three flow rates. The sedimentation of particles is proportional to the concentration ratio of NFs and hybrid NFs. The lower concentration at high flow rate bounces minimum sedimentation than the high concentration at high flow rates. Also, to avoid amalgamation and ensure stability, NFs and hybrid NFs were re-blended and homogenized every morning.

Uncertainty analysis

Uncertainty analysis is necessary to obtain refined data by eliminating outliers. Thermal efficiency uncertainty in the system is calculated by the root sum square method (Akhtar et al., 2020).

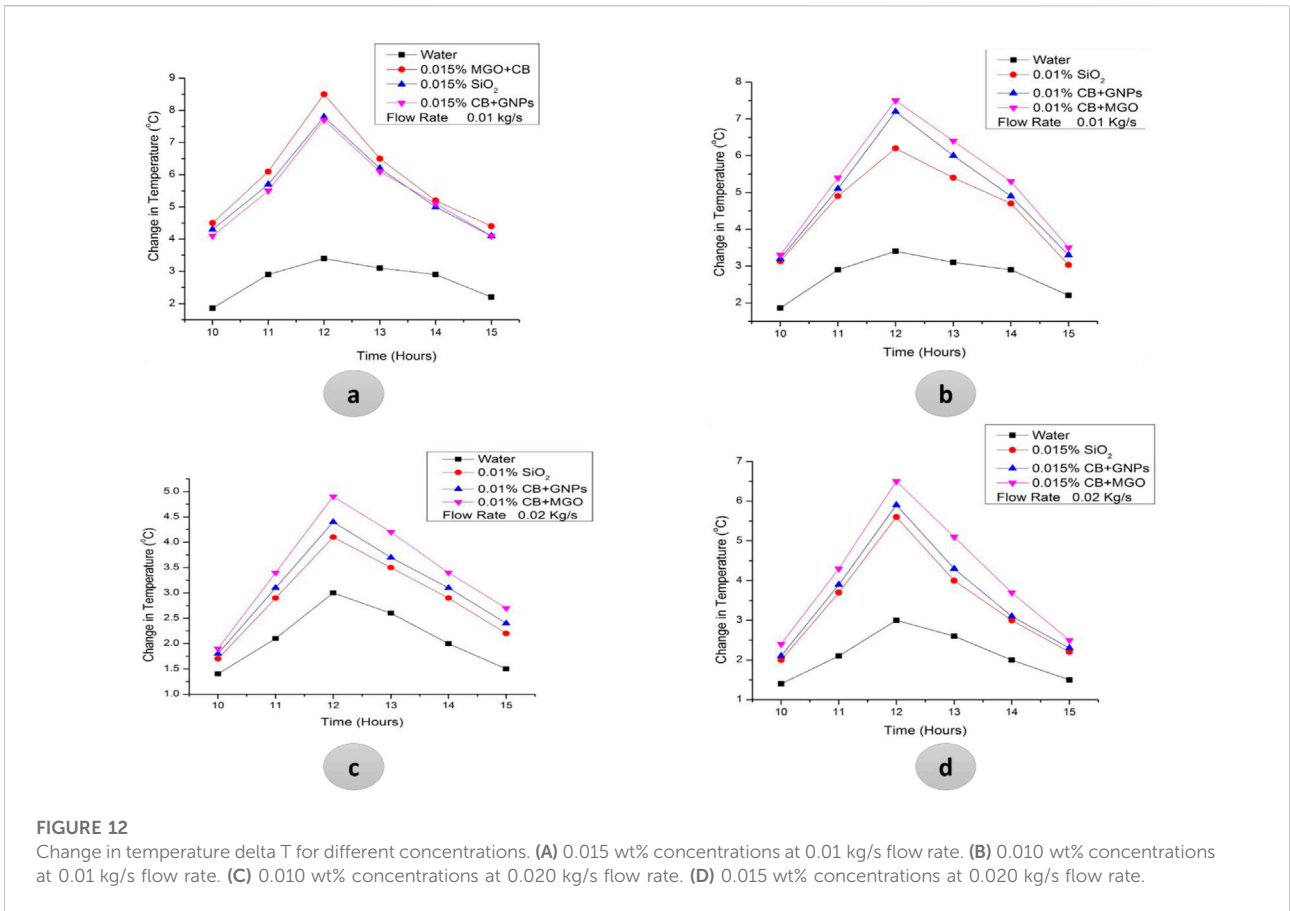$$\alpha = f\ (b_1, b_2, b_3.........), \qquad (4)$$

FIGURE 12
Change in temperature delta T for different concentrations. **(A)** 0.015 wt% concentrations at 0.01 kg/s flow rate. **(B)** 0.010 wt% concentrations at 0.01 kg/s flow rate. **(C)** 0.010 wt% concentrations at 0.020 kg/s flow rate. **(D)** 0.015 wt% concentrations at 0.020 kg/s flow rate.
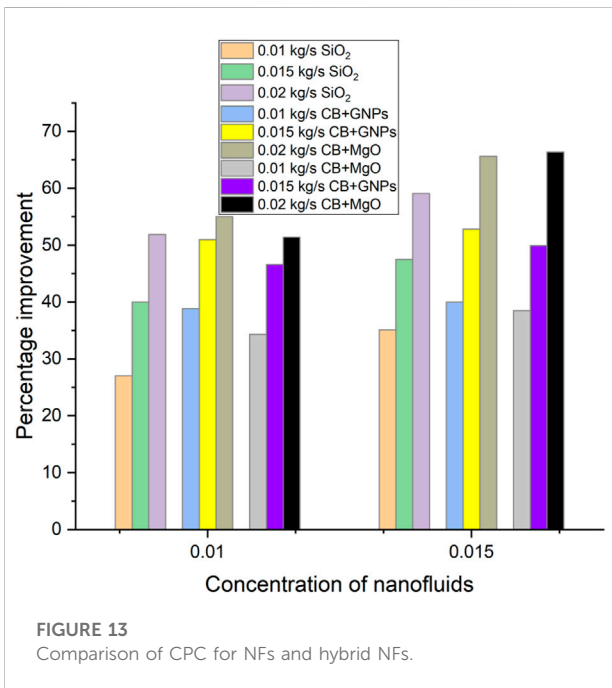

FIGURE 13
Comparison of CPC for NFs and hybrid NFs.

$$\mathrm{c}_\alpha = \sqrt{\left(\frac{\delta\alpha}{\delta b_1}.\mathrm{c}b_1\right)^2 + \left(\frac{\delta\alpha}{\delta b_2}.\mathrm{c}b_2\right)^2 + \left(\frac{\delta\alpha}{\delta b_3}.\mathrm{c}b_3\right)^2 \ldots \quad .} \tag{5}$$

Uncertainty for the thermal efficiency is calculated as around 3.5%.

Conclusion

In the present work, the thermal enhancement of CPCs using NFs and hybrid NFs as heat transfer fluids was investigated. The results of temperature difference of receiver were increased with high particle concentrations and reduced with high flow rates. In all scenarios, efficiencies of CPCs using NFs and hybrid NFs were higher than those of CPCs using base fluid (water). The highest thermal efficiency achieved by experimentation is 66.3% for MgO + CB pair at the highest flow rate and the highest concentration of nanoparticles (0.020 kg/s and 0.015 wt%). Maximum efficiency gain by water at the highest flow rate (0.020 kg/s) is 34.8% under similar experimental conditions. In short, it is concluded as follows:

• Efficiency is calculated by using four types of fluids (water, SiO_2/H_2O + EG (50:50), CB + $GNPs/H_2O$, and MgO + CB/H_2O) at different flow rates and volumetric concentrations of nanoparticles.

• By using water as working fluid variations in temperature difference, heat gain and thermal efficiency are observed from 3.4°C to 1.4°C, 77.8 to 252 W, and 12.5% to 34.8% from the lowest to the highest flow rate.

• By using hybrid base fluid (water and ethylene glycol) and nanoparticles of SiO_2, maximum temperature difference was attained at the lowest flow rate and the highest concentration is 7.8°C, and variations in temperature difference, heat gain, and thermal efficiency are observed from 7.8°C to 2°C, 140.2 to 446.3 W, and 12.8% to 59.13% from the lowest to the highest flow rate and volumetric concentrations.

• By using a hybrid of two non-metallic CB + GNPs in the base fluid of water, maximum temperature difference was attained at the lowest flow rate and the highest concentration is 7.7°C, and variations in temperature difference, heat gain, and thermal efficiency are observed from 7.7°C to 2.1°C, 94.6 to 488.4 W, and 14.2% to 65.68% from the lowest to the highest flow rate and volumetric concentration of the non-metallic pair.

• Thermal enhancement of CPSC is improved by using NFs and optimum results are achieved by using hybrid NFs.

• The increasing behavior of temperature difference and solar heat gain is different at the same flow rates.

• By using various combinations of hybrid NFs, one optimized hybrid NF can be used to obtain optimum results.

• The optimum temperature difference attained by MgO + CB is 8.5°C for the lowest flow rate and the highest concentration of nanoparticles and variations in temperature difference, heat gain, and thermal efficiency are observed from 8.5°C to 2.4°C, 101.5 to 495 W, and 15.3% to 66.3%. The hybrid NFs gave 31.5% improved results than water. The hybrid NFs are more suitable to improve the thermal output of solar collectors. The presented results of experimentations are beneficial for low–medium range industrial applications of CPCs using hybrid NFs.

In the present research work, experimentation is presented by using NFs and different hybrid NFs of metallic and non-metallic hybrid, non-metallic hybrid, and hybrid base fluid using metallic hybrid pair and non-metallic hybrid pair.

• Earlier work was done using CuO and Al_2O_3 NFs with a compound parabolic collector. In the present work, all thermal analyses were performed by using NFs and hybrid NFs. In the future, other types of hybrid NFs may be used to improve the thermal performance of CPC for low–medium range temperature applications.

• CPC thermal performance can also be increased by utilizing metallic hybrid in hybrid base fluids.

• The use of different pairs of hybrid base fluids for metal and non-metal hybrid nanoparticles can lead to a novel work.

Data availability statement

The original contributions presented in the study are included in the article/Supplementary Material; further inquiries can be directed to the corresponding author.

Author contributions

MF: contributed as investigation, writing orignal draft. MIS: Writing draft, and investigation. FJ: writing—review and editing. MU: formal analysis. MM: writing—review and editing, software, and resources. MWS: writing—review and editing. SN: validation. SS: data curation. AY: writing—review and editing. MM: writing—review and editing, and funding acquisition. AE-S: writing—review and editing.

Conflict of interest

The authors declare that the research was conducted in the absence of any commercial or financial relationships that could be construed as a potential conflict of interest.

Publisher's note

All claims expressed in this article are solely those of the authors and do not necessarily represent those of their affiliated organizations, or those of the publisher, the editors, and the reviewers. Any product that may be evaluated in this article, or claim that may be made by its manufacturer, is not guaranteed or endorsed by the publisher.

References

Acosta-Herazo, R., Valadés-Pelayo, P. J., Mueses, M. A., Pinzón-Cárdenas, M. H., Arancibia-Bulnes, C., and Machuca-Martínez, F. (2020). An optical and energy absorption analysis of the solar compound parabolic collector photoreactor (CPCP): The impact of the radiation distribution on its optimization. *Chem. Eng. J.* 395, 125065. doi:10.1016/j.cej.2020.125065

Ahmadi, A., Das, B., Ehyaei, M. A., Esmaeilion, F., El Haj Assad, M., Jamali, D. H., et al. (2021). Energy, exergy, and techno-economic performance analyses of solar dryers for agro products: A comprehensive review. *Sol. Energy* 228, 349–373. doi:10.1016/j.solener.2021.09.060

Ahmadi, M. H., Baghban, A., Sadeghzadeh, M., Zamen, M., Mosavi, A., Shamshirband, S., et al. (2020). Evaluation of electrical efficiency of photovoltaic thermal solar collector. *Eng. Appl. Comput. Fluid Mech.* 14, 545–565. doi:10.1080/19942060.2020.1734094

Akhtar, F., Ali, M., Sheikh, N. A., and Shehryar, M. (2020). Experimental investigation of solar compound parabolic collector using Al2O3/H2O nanofluid in a subtropical climate. *Therm. Sci.* 25, 201. doi:10.2298/TSCI191207201A

Al-Waeli, A. H. A., Sopian, K., Chaichan, M. T., Kazem, H. A., Ibrahim, A., Mat, S., et al. (2017). Evaluation of the nanofluid and nano-PCM based photovoltaic thermal (PVT) system: An experimental study. *Energy Convers. Manag.* 151, 693–708. doi:10.1016/j.enconman.2017.09.032

Allahyar, H. R., Hormozi, F., and ZareNezhad, B. (2016). Experimental investigation on the thermal performance of a coiled heat exchanger using a new hybrid nanofluid. *Exp. Therm. Fluid Sci.* 76, 324–329. doi:10.1016/j.expthermflusci.2016.03.027

Amjad, M., Gardy, J., Hassanpour, A., and Wen, D. (2018). Novel draw solution for forward osmosis based solar desalination. *Appl. Energy* 230, 220–231. doi:10.1016/j.apenergy.2018.08.021

Amjad, M., Raza, G., Xin, Y., Pervaiz, S., Xu, J., Du, X., et al. (2017). Volumetric solar heating and steam generation via gold nanofluids. *Appl. Energy* 206, 393–400. doi:10.1016/j.apenergy.2017.08.144

Amjad, M., Yang, Y., Raza, G., Gao, H., Zhang, J., Zhou, L., et al. (2017). Deposition pattern and tracer particle motion of evaporating multi-component sessile droplets. *J. Colloid Interface Sci.* 506, 83–92. doi:10.1016/j.jcis.2017.07.025

Ayompe, L. M., Duffy, A., McCormack, S. J., and Conlon, M. (2011). Validated TRNSYS model for forced circulation solar water heating systems with flat plate and heat pipe evacuated tube collectors. *Appl. Therm. Eng.* 31, 1536–1542. doi:10.1016/j.applthermaleng.2011.01.046

Babar, H., and Ali, H. M. (2019). Towards hybrid nanofluids: Preparation, thermophysical properties, applications, and challenges. *J. Mol. Liq.* 281, 598–633. doi:10.1016/j.molliq.2019.02.102

Belkhode, P. N., Shelare, S. D., Sakhale, C. N., Kumar, R., Shanmugan, S., Soudagar, M. E. M., et al. (2021). Performance analysis of roof collector used in the solar updraft tower. *Sustain. Energy Technol. Assessments* 48, 101619. doi:10.1016/j.seta.2021.101619

Bellos, E., Korres, D., Tzivanidis, C., and Antonopoulos, K. A. (2016). Design, simulation and optimization of a compound parabolic collector. *Sustain. Energy Technol. Assessments* 16, 53–63. doi:10.1016/j.seta.2016.04.005

Bellos, E., and Tzivanidis, C. (2019). A review of concentrating solar thermal collectors with and without nanofluids. *J. Therm. Anal. Calorim.* 135, 763–786. doi:10.1007/s10973-018-7183-1

Bellos, E., and Tzivanidis, C. (2018). Thermal analysis of parabolic trough collector operating with mono and hybrid nanofluids. *Sustain. Energy Technol. Assessments* 26, 105–115. doi:10.1016/j.seta.2017.10.005

Bhalla, V., and Khullar, V. (2021). *Design and thermal analysis of nanofluid-based compound parabolic concentrator.*

Campos, C., Vasco, D., Angulo, C., Burdiles, P. A., Cardemil, J., and Palza, H. (2019). About the relevance of particle shape and graphene oxide on the behavior of direct absorption solar collectors using metal based nanofluids under different radiation intensities. *Energy Convers. Manag.* 181, 247–257. doi:10.1016/j.enconman.2018.12.007

Chen, M., He, Y., Huang, J., and Zhu, J. (2016). Synthesis and solar photo-thermal conversion of Au, Ag, and Au-Ag blended plasmonic nanoparticles. *Energy Convers. Manag.* 127, 293–300. doi:10.1016/j.enconman.2016.09.015

Chen, N., Ma, H., Li, Y., Cheng, J., Zhang, C., Wu, D., et al. (2017). Complementary optical absorption and enhanced solar thermal conversion of CuO-ATO nanofluids. *Sol. Energy Mater. Sol. Cells* 162, 83–92. doi:10.1016/j.solmat.2016.12.049

Crisostomo, F., Hjerrild, N., Mesgari, S., Li, Q., and Taylor, R. A. (2017). A hybrid PV/T collector using spectrally selective absorbing nanofluids. *Appl. Energy* 193, 1–14. doi:10.1016/j.apenergy.2017.02.028

Dimri, N., Tiwari, A., and Tiwari, G. N. (2018). Effect of thermoelectric cooler (TEC) integrated at the base of opaque photovoltaic (PV) module to enhance an overall electrical efficiency. *Sol. Energy* 166, 159–170. doi:10.1016/j.solener.2018.03.030

Esfe, M. H., Esfandeh, S., Saedodin, S., and Rostamian, H. (2017). Experimental evaluation, sensitivity analyzation and ANN modeling of thermal conductivity of ZnO-MWCNT/EG-water hybrid nanofluid for engineering applications. *Appl. Therm. Eng.* 125, 673–685.

Esfe, M. H., Wongwises, S., Naderi, A., Asadi, A., Safaei, M. R., Rostamian, H., et al. (2015). Thermal conductivity of Cu/TiO2–water/EG hybrid nanofluid: Experimental data and modeling using artificial neural network and correlation. *Int. Commun. Heat. Mass Transf.* 66, 100–104.

Farajzadeh, E., Movahed, S., and Hosseini, R. (2018). Experimental and numerical investigations on the effect of Al2O3/TiO2H2O nanofluids on thermal efficiency of the flat plate solar collector. *Renew. Energy* 118, 122–130. doi:10.1016/j.renene.2017.10.102

Ghafoor, D. A., Rehman, T., Munir, A., Ahmad, M., and Iqbal, M. (2016). Current status and overview of renewable energy potential in Pakistan for continuous energy sustainability. *Renew. Sustain. Energy Rev.* 60, 1332–1342. doi:10.1016/j.rser.2016.03.020

Gilani, H. A., and Hoseinzadeh, S. (2021). Techno-economic study of compound parabolic collector in solar water heating system in the northern hemisphere. *Appl. Therm. Eng.* 190, 116756.

Hachicha, A. A., Rodríguez, I., Capdevila, R., and Oliva, A. (2013). Heat transfer analysis and numerical simulation of a parabolic trough solar collector. *Appl. Energy* 111, 581–592. doi:10.1016/j.apenergy.2013.04.067

Hamid, K. A., Azmi, W. H., Nabil, M. F., and Mamat, R. (2018). Experimental investigation of nanoparticle mixture ratios on TiO2-SiO2 nanofluids heat transfer performance under turbulent flow. *Int. J. Heat Mass Transf.* 118, 617–627. doi:10.1016/j.ijheatmasstransfer.2017.11.036

Harrabi, I., Hamdi, M., and Hazami, M. (2021). Long-term performances and technoeconomic and environmental assessment of Al2O3/water and MWCNT/oil nanofluids in three solar collector technologies. *J. Nanomater.* 2021. doi:10.1155/2021/6461895

Hjerrild, N. E., Mesgari, S., Crisostomo, F., Scott, J. A., Amal, R., and Taylor, R. A. (2016). Hybrid PV/T enhancement using selectively absorbing Ag-SiO 2/carbon nanofluids. *Sol. Energy Mater. Sol. Cells* 147, 281–287. doi:10.1016/j.solmat.2015.12.010

Jiang, C., Yu, L., Yang, S., Li, K., Wang, J., Lund, P. D., et al. (2020). A review of the compound parabolic concentrator (CPC) with a tubular absorber. *Energies* 13, 695. doi:10.3390/en13030695

Khalil, A., Amjad, M., Noor, F., Hussain, A., Nawaz, S., Filho, E. P. B., et al. (2020). Performance analysis of direct absorption-based parabolic trough solar collector using hybrid nanofluids. *J. Braz. Soc. Mech. Sci. Eng.* 42, 573. doi:10.1007/s40430-020-02654-2

Kim, Y. S., Balkoski, K., Jiang, L., and Winston, R. (2013). Efficient stationary solar thermal collector systems operating at a medium-temperature range. *Appl. Energy* 111, 1071–1079. doi:10.1016/j.apenergy.2013.06.051

Korres, D., Bellos, E., and Tzivanidis, C. (2019). Investigation of a nanofluid-based compound parabolic trough solar collector under laminar flow conditions. *Appl. Therm. Eng.* 149, 366–376. doi:10.1016/j.applthermaleng.2018.12.077

Korres, D., and Tzivanidis, C. (2018). A new mini-CPC with a U-type evacuated tube under thermal and optical investigation. *Renew. Energy* 128, 529–540. doi:10.1016/j.renene.2017.06.054

Leong, K. Y., Razali, I., Ku Ahmad, K. Z. K., Ong, H. C., Ghazali, M. J., and Abdul Rahman, M. R. A. (2018). Thermal conductivity of an ethylene glycol/water-based nanofluid with copper-titanium dioxide nanoparticles: An experimental approach. *Int. Commun. Heat Mass Transf.* 90, 23–28. doi:10.1016/j.icheatmasstransfer.2017.10.005

Li, Q., Zheng, C., Shirazi, A., Bany Mousa, O. B., Moscia, F., Scott, J. A., et al. (2017). Design and analysis of a medium-temperature, concentrated solar thermal collector for air-conditioning applications. *Appl. Energy* 190, 1159–1173. doi:10.1016/j.apenergy.2017.01.040

Menbari, A., Alemrajabi, A. A., and Ghayeb, Y. (2016). Experimental investigation of stability and extinction coefficient of Al 2 O 3 -CuO binary nanoparticles dispersed in ethylene glycol-water mixture for low-temperature direct absorption solar collectors. *Energy Convers. Manag.* 108, 501–510. doi:10.1016/j.enconman.2015.11.034

Menbari, A., Alemrajabi, A. A., and Rezaei, A. (2017). Experimental investigation of thermal performance for direct absorption solar parabolic trough collector (DASPTC) based on binary nanofluids. *Exp. Therm. Fluid Sci.* 80, 218–227. doi:10.1016/j.expthermflusci.2016.08.023

Oloketuyi, I. S., Ajide, O. O., Odesola, F. I., Oyewola, O. M., and Adaramola, M. S. (2020). Examination of heat transfer performance of a nonimaging hybrid compound parabolic collector in low latitude and cloudy region. *Environ. Prog. Sustain. Energy* 39, e13339. doi:10.1002/ep.13339

Parsian, A., and Akbari, M. (2018). New experimental correlation for the thermal conductivity of ethylene glycol containing Al2O3-Cu hybrid nanoparticles. *J. Therm. Anal. Calorim.* 131, 1605–1613. doi:10.1007/s10973-017-6694-5

Qamar, A., Arshad, A., Anwar, Z., Shaukat, R., Amjad, M., Imran, S., et al. (2021). Dispersion stability and rheological characteristics of water and ethylene glycol based ZnO nanofluids. *Therm. Sci.* 25.

Sathieshkumar, N. (2018). Performance analysis of hybrid solar photovoltaic thermal collector with nanoparticles. *Int. J. Curr. Res. Eng. Technol.* 1, 6–11.

Snail, K. A., O'Gallagher, J. J., and Winston, R. (1984). A stationary evacuated collector with integrated concentrator. *Sol. Energy* 33, 441–449. doi:10.1016/0038-092X(84)90196-8

Subramani, J., Nagarajan, P. K., Mahian, O., and Sathyamurthy, R. (2018). Efficiency and heat transfer improvements in a parabolic trough solar collector using TiO2 nanofluids under turbulent flow regime. *Renew. Energy* 119, 19–31. doi:10.1016/j.renene.2017.11.079

Sundar, L. S., Singh, M. K., and Sousa, A. C. M. (2014). Enhanced heat transfer and friction factor of MWCNT-Fe3O4/water hybrid nanofluids. *Int. Commun. Heat Mass Transf.* 52, 73–83. doi:10.1016/j.icheatmasstransfer.2014.01.012

Suresh, S., Venkitaraj, K. P., Selvakumar, P., and Chandrasekar, M. (2011). Synthesis of Al2O3-Cu/water hybrid nanofluids using two step method and its thermo physical properties. *Colloids Surfaces A Physicochem. Eng. Aspects* 388, 41–48. doi:10.1016/j.colsurfa.2011.08.005

Takabi, B., and Salehi, S. (2014). Augmentation of the heat transfer performance of a sinusoidal corrugated enclosure by employing hybrid nanofluid. *Adv. Mech. Eng.* 6, 147059. doi:10.1155/2014/147059

Tiwari, S., and Tiwari, G. N. (2017). Thermal analysis of photovoltaic thermal integrated greenhouse system (PVTIGS) for heating of slurry in potable biogas plant: An experimental study. *Sol. Energy* 155, 203–211. doi:10.1016/j.solener.2017.06.021

Toghraie, D., Chaharsoghi, V. A., and Afrand, M. (2016). Measurement of thermal conductivity of ZnO-TiO2/EG hybrid nanofluid. *J. Therm. Anal. Calorim.* 125, 527–535. doi:10.1007/s10973-016-5436-4

Verma, S. K., Tiwari, A. K., Tiwari, S., and Chauhan, D. S. (2018). Performance analysis of hybrid nanofluids in flat plate solar collector as an advanced working fluid. *Sol. Energy* 167, 231–241. doi:10.1016/j.solener.2018.04.017

Vijayakumar, P., Kumaresan, G., Gokul Kumar, S. G., and Eswaran, M. (2021). A review on applications of nanofluid in evacuated tube heat pipe integrated with compound parabolic concentrator. *Mater. Today Proc.* 45, 1227–1232. doi:10.1016/j.matpr.2020.04.250

Wang, X., He, Y., Chen, M., and Hu, Y. (2018). ZnO-Au composite hierarchical particles dispersed oil-based nanofluids for direct absorption solar collectors. *Sol. Energy Mater. Sol. Cells* 179, 185–193. doi:10.1016/j.solmat.2017.11.012

Xu, Z. Y., and Wang, R. Z. (2017). Comparison of CPC driven solar absorption cooling systems with single, double and variable effect absorption chillers. *Sol. Energy* 158, 511–519. doi:10.1016/j.solener.2017.10.014

Younis, A., Elsarrag, E., Alhorr, Y., and Onsa, M. (2018). The influence of Al2O3-ZnO-H2O nanofluid on the thermodynamic performance of photovoltaic-thermal hybrid solar collector system. *Innov. Ener Res.* 7, 1463–2576. doi:10.4172/2576-1463.1000187

Zeng, J., Xuan, Y., and Duan, H. (2016). Tin-silica-silver composite nanoparticles for medium-to-high temperature volumetric absorption solar collectors. *Sol. Energy Mater. Sol. Cells* 157, 930–936. doi:10.1016/j.solmat.2016.08.012

Zeng, J., and Xuan, Y. (2018). Enhanced solar thermal conversion and thermal conduction of MWCNT-SiO2/Ag binary nanofluids. *Appl. Energy* 212, 809–819. doi:10.1016/j.apenergy.2017.12.083

Nomenclature

Symbols

^{A}r Receiver area (m^2)

^{A}a Aperture area (m^2)

A Aperture width (m)

Au Gold

Ag Silver

Al$_2$O$_3$ Alumina

Cp Specific heat capacity (J/kg.K)

CPSC Compound parabolic solar collector

CB Carbon black

CuO Copper oxide

DASC Direct absorption solar collector

EG Ethylene glycol

FPSC Flat plate solar collector

HCPC Hybrid compound parabolic collector

HVAC Heating, ventilation, and air conditioning

H$_2$O Water

GNPs Graphene nanoplatelets

G$_e$ Solar irradiance (W/m^2)

m' Mass flow rate (kg/s)

MgO Magnesium oxide

MWCNTs Multiwall carbon nanotubes

PV/T Photovoltaic/thermal

PTC Parabolic trough collector

^{Q}u Solar heat gain (W)

Q_s Energy potential (W)

ΔT Temperature difference (°C)

^{T}a Ambient temperature (°C)

^{Tc} Collector temperature (°C)

^{Ti} Inlet temperature (°C)

TiO$_2$ Titania

SiO$_2$ Silica

Greek letters

η$_{th}$ Thermal efficiency